International Journal of Occupational Medicine and Environmental Health, Vol. 12, No 4, 305–330, 1999

EVALUATION OF DOSES TO PATIENTS IN X-RAY DIAGNOSTICS IN POLAND

MARIA ANNA STANISZEWSKA

Department of Radiological Protection
The Nofer Institute of Occupational Medicine
Łódź, Poland

Key words: X-ray diagnostics, Examinations, Patients, Doses

Abstract. The study includes a detailed analysis of patients' exposure to ionising radiation resulting from diagnostic radiology in Poland. Data concerning the number and types of examinations were collected by wide-range questionnaire surveys conducted in 1986 and 1995. As the result, the number of examinations per 1000 inhabitants was found to be 572 in 1986 and 715 in 1995. Most of the examinations were the basic, conventional ones (mostly chest and spine radiography).

A great part of this study includes detailed description of the methodology of evaluating doses received by patients from X-ray procedures. The theoretical Monte Carlo simulation with the original author's computer code was used for this purpose.

As the result, the doses to patients in six age groups (<1, 1–4, 5–9, 10–14, 15–19 and the adults) were estimated. In simulation process the examined persons were represented by the appropriate mathematical human phantoms.

The doses from particular examinations performed in exposure conditions routinely used in Polish radiology departments are presented. The mean effective doses for adult patients from typical examinations are: 0.11 mSv from chest, 3.0 mSv from thoracic spine, and 4.3 mSv from L-S spine radiography.

Significantly higher doses were received by patients undergoing fluoroscopy procedures: 23 mSv from barium enema and 14 mSv from the stomach examination.

In conclusion, the estimated exposure levels in Poland are as follows:

– the average effective dose per examination: (1.4±0.6) mSv in 1986, (1.2±0.5) mSv in 1995,
– the average effective dose *per capita*: (0.8±0.3) mSv in 1986 and 1995.

INTRODUCTION

Diagnostic radiology of today offers the multifarious possibilities, including various types of imaging, sizes of irradiated body areas, time of exposure, etc. These developments have contributed greatly to the advancement in diagnostic procedures, but in consequence they diversified the radiation dose to the population from

Address reprint requests do Dr. MA Staniszewska, Department of Radiological Protection, The Nofer Institute of Occupational Medicine, P.O. Box 199, 90-950 Łódź, Poland.

medical X-ray examinations. Although conventional X-ray examinations are most frequent in routine practice, technical innovations like computed tomography, digital fluoroscopy, etc., have evoked a growing interest in clinical use of X-ray diagnostic examinations over recent years.

Therefore, X-ray diagnostics has become responsible for increasing exposure of the general population to ionising radiation in highly industrialised and developed countries. Trying to analyse this problem, wide-range surveys are repeated every few years in a number of countries to evaluate current levels of average dose per capita resulting from this source of radiation.

The problem of exposure caused by X-ray diagnostics is important also in Poland, where annually over 26 million of examinations are performed.

The main aim of this study was to evaluate doses received by patients, taking account of the structure of examinations and the age of patients.

MATERIALS AND METHODS

For the estimation of doses from particular X-ray examinations, it was necessary to define typical exposure conditions in common X-ray procedures, including projections and age groups (about 100 (!) various combinations), for which absorbed organ doses, and consequently effective doses were supposed to be evaluated.

Since children and adolescents should also be covered by this analysis, the experimental methods for estimating absorbed organ doses had to be rejected, as adequate physical children phantoms are not available.

A theoretical method based on the Monte Carlo simulation was chosen for this purpose as the only one which allows to analyse such a great number of exposure conditions, and a new, original computer code was developed by the author.

MATHEMATICAL PHANTOM

A series of Cristy phantoms (3) was taken in this study as the basic scheme for defining persons at different age, exposed to X-ray examinations, although the upper part of trunk in these phantoms is highly mathematized, and thus, decreasing their anatomical representativenes (this mainly concerns the shape of lungs and ribs: the bridge is not separated, and all ribs are closed and placed parallelly to the base of the trunk, like the base of the lungs). If such a simplified phantom construction is exposed to an external X-ray beam one can expect that the distribution of absorbed energies resulting from the simulation will significantly differ from that possible for a person with a standard body construction.

The difference is due to:

– an unnaturally enlarged surface of ribs; this results in a higher amount of energy absorbed by skeleton as a whole,

– an unnatural shielding of lungs by closed rings of ribs, decreasing absorption in the lungs,

– the closed rings of ribs in the area of diaphragm which can deform the process of photon scattering and change doses absorbed in the organs situated in the upper abdomen.

Bearing this in mind, a modified version of Cristy phantoms was developed by the author to introduce necessary changes in the construction of the ribs, lungs and the heart. A detailed description of these phantoms together with the comparison of organ doses between the original and modified versions has been presented elsewhere (10).

COMPUTER CODE

The computer code for organ doses calculations consists of:

(a) the main simulation programme (MONT),

(b) the programme to summarize the absorbed energies and compute standard errors of these energies for specified parts of phantoms (NSUM),

(c) the programme to compute the absorbed doses in specified parts of phantoms (representing particular organs) (NDOS).

The computations were carried out using IBM compatible computer with a Turbo Pascal compiler. In each simulation cycle, 6 105 histories of individual photons were followed.

The main simulation programme (MONT)

MONT computes the values of energy absorbed in specified parts of a phantom as a result of X-ray beam transfer. X-ray beam consisted of N quanta (photons) with specified physical characteristics and geometry of incidence.

Each X-ray examination was described by the following exposure parameters:

- anatomical localisation, shape and sizes of x-ray beam incidence area,
- source-skin distance (measured along the central ray),
- X-ray tube current and voltage, combined with total filtration value.

These parameters are input data necessary to start the simulation programme. In addition, the number specific to the mathematical phantom, representing a given age group, and its anatomical data stored in the computer memory is used.

The implementation of the MONT programme begins with INCID procedure, which finds cartesian co-ordinates and directional angles of each photon entering into the phantom.

Primary energy of incident photon is stochastically chosen from an appropriate spectrum determined by values of kilovoltage and filtration. (The catalogue consisting of 48 diagnostic spectra according to Seelentag (7) is also stored in the computer memory.)

The main simulation process starts when the photon (with determined energy, co-ordinates and direction of motion) enters into the phantom. This is performed through the following sequence of procedures:

(1) the finding of an average free path of the photon and its movement towards the known direction;

(2) the computation of new (actual) co-ordinates of the photon (in the stationary co-ordinate system connected with phantom);

(3) the determination of organ inside of which the photon actually 'stopped';

(4) the stochastic choice of an interaction process as the most probable for the photon with given energy in the medium having physical properties (i.e. absorption coefficient) of a given organ; if Compton scattering or photo-effect is most probable, the fraction of photon energy lost during the process is stored in the organ in which the interaction has occurred;

(5) the decision about further follow-up of the photon history;

(a) in the case of positive decision the programme returns to procedure (1),

(b) the negative decision is taken if:

(i) the energy of the photon is lower than 4 keV,

(ii) the photo-effect occurred and the whole energy is absorbed at the site of interaction,

(iii) the photon went beyond the outer surface of the phantom.

The history of each quantum is investigated independently. This means that the sequence of procedures (1)–(5) is repeated at least N times. (N is the number of photons in simulation.) Possible returns to ealier procedures (recurrence) during an analysis of a given photon is not taken into account.

The results presented in this paper were obtained for $N = 6 \cdot 10^5$ photons. Energies stored in specified parts of the phantom are summarised and recorded after each portion of $\frac{N}{20}$ $(3 \cdot 10^4)$ photons passed through the phantom; hence, the final file of results is composed of 20 records being totally independent of each other.

The data on the exposure parameters routinely used in X-ray examinations were collected from 66 radiology departments (in 13 voivodships of Poland), performing a wide spectrum of examinations, by qualified specialists in radiological protection of regional sanitary and epidemiological stations.

The obtained data were divided according to types of examinations and the age groups of patients.

To verify correctness of the basic algorithm used in MONT programme the following simulation test was performed: a thin soft tissue slab ($100 \cdot 100$ cm) was exposed to a narrow beam ($10 \cdot 10$ cm) of monoenergetic photons ($30 \cdot 10^4$ of 30 keV photons), aimed at the centre of the slab from the source-slab distance of 200 cm.

The thickness corresponding to 0.5 HVL, 1 HVL and 2 HVL for a soft tissue at 30 keV was chosen for a simplified phantom; the theoretically expected values of intensities for transmitting photons were 50%, 71% and 25%, respectively. The results of simulation for this slab were 53%, 70% and 30%, respectively.

Because of non-uniform density of human mathematical phantom it is impossible to predict results of simulation, hence the obtained results were adopted as a first order proof of the simulation algorithm correctness.

Summarising programme (NSUM)

NSUM is based on MONT results and the following conversion is done:

(a) the energies absorbed in specified parts of the phantom (organs) as a result of interaction of each successive portion $\frac{N}{20}$ photons are summed up to obtain the values yielded by the whole number (N) of photons in the simulation process;

(b) standard error of energy absorbed in particular organ 'i' (SEi) is computed:

$$SE_i = \sqrt{\frac{\sum_j X^2 - n_x^{-2}}{n}}$$

where: x_i – the energy absorbed in 'i' organ as a result of interaction of 'j' portion of $\frac{N}{20}$ photons; j – 1 ... 20; n = 20.

For the organ in which absorption occurred for only one portion of $\frac{N}{20}$ photons, as a rule, the standard error equalling the absorbed energy was adopted. The final product of NSUM is the file including both absorbed energies and standard errors for all specified parts of the phantom.

Transition from simulation conditions to a real examination under study

As mentioned above, the results of NSUM are referred to a number of photons in the simulation process; obviously, the number of photons emitted by X-ray tube in real conditions is much higher. Consequently, the values of absorbed energies are also higher, proportionally to the ratio of the real number of emitted photons to that in simulation ($N = 6 \cdot 10^5$). This ratio (called 'multiplication factor') can be determined for photons with the same energy spectrum and geometry of incidence. Knowledge of this quotient is necessary for calculation of absorbed doses from external exposure if the real number of photons differs from that assumed for the simulation.

The most simple solution of this problem is to count photons emitted by X-ray tube during real examinations. Possible differences in the emission efficiency of a particular X-ray generator with the same parameters should be taken into consideration. Since this solution is impossible for obvious practical reasons, the author of this paper **elaborated a new original method** for evaluating the average **'multiplication factor'**.

This method is based on determination of theoretical relation between the entrance air kerma (AK) and the number of photons in the primary X-ray beam (N). Since

$$AK = C \cdot N,$$

where: C – proportionality coefficient related to physical characteristics of X-rays, the following relations are true, if this characteristics does not change:

$$\frac{N_1}{N_2} = \frac{AK_1}{AK_2} = \frac{D_1}{D_2}$$

where: AK_i – AK evaluated at a constant point, where the beam enters the phantom consisting of N_i – photons, D_i – a dose absorbed in a specified constant object exposed to AK_i (i = 1,2).

These relations also mean that:

$$D_2 = \left(\frac{D_1}{AK_1}\right) \cdot AK_2$$

If N_1 is the number of photons in simulation, and N_2 denotes a number of photons emitted in real conditions of examination, then the $\frac{N_1}{N_2}$ ratio is called a 'multiplication factor'.

The aforesaid relations pose a serious problem: values of N_1 and AK_2 are known (from the assumption and from the measurement, respectively), contrary to AK_1 and N_2. In short, the relation between AK and N is unknown. Without knowing this relation the 'multiplication factor' cannot be evaluated, which indicates the lack of the **prerequisite** for any further computation of absorbed doses.

This issue has not as yet been discussed either in publications of the National Radiological Protection Board (NRPB), or Gessellschaft fur Strahlen- und Umwelt-forschung mbH (GSF) reports (4,5) or in the ealier ones (1,6).

If this problem could be solved, on the basis of the above equation it would be possible to compute 'conversion coefficients' (D/AK, (mGy/mGy)), very useful for evaluating doses in real examination for which air kerma (AK_e) is known, owing to the results of Monte Carlo simulation given as $(D/AK)_s$, i.e. $D_e = (D/AK)_s \cdot AK_e$.

To this end, the following conditions have to be fulfilled:

(a) physical quality of X-rays should not differ significantly between simulation and real examination under study,

(b) the number of photons in the simulation process must be large enough.

Since the solution to the problem discussed was essential to performing this study, the author developed an original method of theoretical evaluation of the air kerma, which also allows to formulate the relationship between the number of photons and the air kerma.

THEORETICAL METHOD FOR THE AIR KERMA EVALUATION IN DIAGNOSTIC X-RAY EXAMINATIONS

Kerma is defined as the quotient of the sum of the initial kinetic energies (ΣE_{kin}) of all the charged ionising particles liberated by uncharged ionising particles in a material of mass 'M', i.e.

$$AK = \frac{\Sigma E_{kin}}{M} \qquad [1]$$

For diagnostic X-ray exposures, the entrance air kerma at a point of incidence of the central ray on patient's body is evaluated (Fig. 1).

The energy of X-ray quanta in primary beam generated by diagnostic units do not exceed 120–130 keV; hence the physical processes responsible for ionisation of air slab which separates X-ray source and patient's body surface are photoeffect and Compton scattering. During both processes, free electron may be produced, but secondary free electrons with kinetic energies, significantly higher than zero, are most

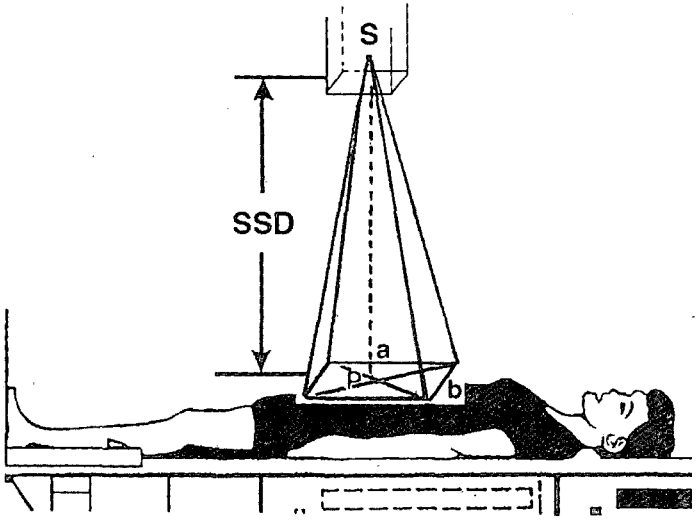

Fig. 1. The scheme of exposure geometry.
S – source of radiation; SSD – source – skin distance; a,b – dimensions of primary beam at incidence plane.

probably released as a result of inelastic scattering. Taking account of the conservation of energy and momentum in Compton effect, the kinetic energy of free electrons is given by

$$Te = E\left[1 - \frac{1}{1 + \frac{E}{mc^2}(1 - \cos\theta)}\right] \qquad [2]$$

where: E – energy of interacting X quant, θ – angle of scattering of X quant, $mc^2 = 511$ keV – rest mass of electron.

The sum of kinetic energies of electrons liberated as a result of transfer of primary beam containing N_x quants through the slab of air is given by

$$\Sigma E_{kin} = N_x \cdot T_e \qquad [3]$$

The above equation [3] is based on the assumption, that all quanta in primary beam have the same value of energy (E), being the mode of energies in X-ray spectrum. This means, that the shape of energy spectrum is neglected. The whole primary beam is treated as monoenergetic, with energy E. The likelihood of both processes of interaction (i.e. photoeffect and inelastic scattering) of X quanta with air is taken into consideration if the coefficient of probability is included into formula [3]:

$$\Sigma E_{kin} = N_x \cdot T_e \cdot \left(\frac{\sigma_c + \sigma_F}{\mu_{att}}\right)\Big|_E \qquad [4]$$

where: σ_c, σ_F – are the cross- section of Compton scattering and photoeffect, respectively, and μ_{att} – attenuation coefficient for air.

All values are taken for the same energy (E) of quanta. Mass of air in the slab which primary X quanta pass through can be estimated as:

$$M = \frac{1}{2}\,SSD\,(a \cdot b) \cdot \varrho_{air} \qquad [5]$$

where: a, b – dimensions of primary beam (Fig. 1), ϱ_{air} – density of air ($\sigma_{air} = 1.29 \cdot 10^{-3}$ g/cm^3).

The number of X quanta emitted by X-ray tube (N_x) is given by

$$N_x = 1.0625 \cdot 10^{12}\,\frac{MAS \cdot U}{E} \cdot \frac{a \cdot b}{(SSD)^2} \cdot \exp\left[-\left(\frac{\mu}{\varrho}\right)_{A1} \cdot \varrho_{A1} \cdot TF\right] \cdot \exp\left[-\left(\frac{\mu}{\varrho}\right)_{air} \cdot \varrho_{air} \cdot SSD\right] \qquad [6]$$

In formula [6] conservation of energy fluence inside the primary beam between the tube focus and the patient's skin is assumed.

The constant coefficient of $1.0625 \cdot 10^{12}$ includes average tube effectiveness ($\eta \cong 1\%$), typical angle of anode declination ($\alpha \cong 17.5°$), and factor resulting from conversion of the number of electrons emitted from cathode into the value of charge passing through the tube.

MAS denotes the product of the anode current and time of exposure.

Regarding all the relationships mentioned above [2–6] AK is defined by the following formula:

$$AK = \frac{N_x \cdot \frac{E^2}{mc^2}\,(1 - \cos\theta) \cdot \left(\frac{\sigma_c + \sigma_F}{\mu_{att}}\right)\Big|_E}{\frac{1}{2}\,SSD\,(a \cdot b) \cdot \varrho_{air}} \qquad [7]$$

As the scattering under the angle close to 30° is most **probable**, this value is assumed to be a constant for all interactions. Thus

$$AK \cong 516 \cdot \frac{E}{(SSD)^3}\,MAS \cdot U \cdot (1 - \cos\theta) \cdot \left(\frac{\sigma_c + \sigma_F}{\mu_{att}}\right)\Big|_E \cdot \exp\left[-\left(\frac{\mu}{\varrho}\right)_{A1} \cdot \varrho_{A1} \cdot TF\right] \cdot \exp\left[-\left(\frac{\mu}{\varrho}\right)_{air} \cdot \varrho_{air} \cdot SSD\right] \qquad [8]$$

The E value is derived individually for X-ray spectrum (designed by kilovoltage and filtration) for which other coefficients are evaluated (cross-sections, mass attenuation coefficients, etc.).

One computer code in Turbo Pascal with two catalogues of data: X-ray spectra, and physical parameters of materials as a function of energy, was used for computations.

The computations start when the number of spectrum in the catalogue is determined. The best results of approximation can be obtained when the real settings of kilovoltage and filtration are nearly the same as those in the X-ray spectrum chosen to the computations.

The AK determining formula [8] was verified by comparing the computed values with the measured ones for given exposure conditions. To this end, 240

measurements of AK were performed. Exposure conditions were chosen as appropriate for thoracic spine, lumbo-sacral spine and chest radiographies, when a standard adult patient is examined (height: 170 cm, body mass: 70 kg).

Different types of X-ray units, most frequently X-18, XD-18 and EDR-750, were used for exposures and thermoluminescent dosemeters (TLD), after calibration with NOMEX (PTW Frieburg) for AK measurements. TLDs were placed in PMMA cassettes (5 · 5 cm) with walls 2 mm thick.

Each cassette contained of 10 TLDs placed during exposure on a 3-cm slab of PMMA, and central ray of X-ray beam entered the centre of the cassette.

The measurement and computed results were compared according to the following formula:

$$R = \frac{AKM - AKO}{AKM} \cdot 100\% \qquad [9]$$

where: AKM – measured AK, AKO – computed AK.

The distribution of differences in results are presented below.

Value of difference (without sign)	Percentage of exposures with differences from given range
(0–5)%	10
(5–10)%	8
(10–20)%	21
(20–30)%	15
(30–40)%	13
(40–50)%	19
(50–60)%	9
(60–70)%	3
(70–90)%	2

The mean value of difference R (without sign) in whole collection of data (240 exposures) is 29%, with standard deviation (SD) of 18%.

Having taken account of the sign of difference R, 58 and 42% of exposures with positive and negative R sign, respectively can be observed. The mean value of difference R (with sign) in the whole collection of the data is +6.5, with SD of 34%.

A larger number of positive differences proves that the values obtained by the proposed method of AK evaluation are slightly underestimated.

For obvious reasons, in this method the following aspects are not considered:

(a) slight differentiation of energy spectrum of primary X-rays emitted from X-ray units with different generation mode (pulses/sec), however it is more significant for absorbed doses than for AK;

(b) divergencies between real values of exposure parameters and those chosen on control panel of X-ray units;

(c) the value of total filtration for some types of X-ray units which were difficult to assess.

These may be responsible for differences between AKM and AKO values.

Despite possible uncertainty, this method seems to be quite suitable for theoretical evaluation of air kerma. It allows to compute an approximate and mean value of AK, based only on the known exposure parameters displayed on the control panels of X-ray units.

RESULTS

Doses received by patients from medical X-ray examinations evaluated by Monte Carlo method

The computations were performed for the following X-ray examinations: chest radiography and photofluorography, spine, abdomen, pelvis and hip joints radiography, urography (IVU), and cystography, stomach and esophagus procedures, barium enema and lung fluoroscopy.

Doses were evaluated in those age groups of patients with significant share in the total number of a given type of examination.

The results obtained for particular mathematical phantoms (representing standard humans aged 0, 1, 5, 10, 15 and adults) were attributed to patients of the following age groups: <1, $1-4$, $5-9$, $10-14$, $15-19$ and the adults.

The computations were made taking account of exposure conditions typical for particular X-ray examinations.

In addition, the results obtained for adult patients undergoing most common X-ray examinations, the doses were also computed for extreme exposure conditions (resulting in minimal and maximal air kerma values).

Special attention was also paid to examinations of children; additional evaluations of doses were performed for chest radiography (AP) and cystourethero-graphy (relatively frequent among children below 10 years) and barium enema in children over 10 years. The appropriate data were taken from the Department of Paediatric Radiology, the Polish Mother Memorial Hospital, Łódź.

Doses absorbed in organs with the highest wT weighting factors: ovaries, testes, red bone marrow (RBM), large intestine (LI), lungs, stomach, breasts and thyroid, are presented in Tables $1-10$ (the following abbreviations are used: AP-anterior-posterior, PA-posterior-anterior, LLAT-left lateral and RLAT-right--laterial). For particular examinations and age groups of patients, projection-related doses are given for specified primary X-ray beams. Examinations with computed doses for extreme conditions are marked: aver-typical and min or max – extremal conditions, respectively.

If the values of absorbed organ doses are known, it is possible to evaluate effective doses received by patients of individual age groups from particular X-ray examinations. Effective doses per unit of the entrance air kerma (in mSv/mGy) for specified projections, and total effective doses per examination together with standard errors are given in Table 11. The presented values apply to typical (average) exposure parameters used in Polish radiological departments.

There is good reason to believe, that these results can be also used for estimating patient doses in slightly different (but known!) exposure conditions, providing that the quality of the primary beam does not differ significantly from that assumed.

Table 1A. Chest radiography in children: organ doses

Age (years)	Projection	Exposure parameters	Average absorbed doses (μGy)							
			Ovaries	Testes	RBM	LI	Lungs	Stomach	Breast	Thyroid
<1	AP	50 kV + 2 mm Al, SSD = 80 cm; 13 · 21	11	<0.1	18	11	64	38	19	59
		70 kV + 3 mm Al, SSD = 78 cm; 13 · 15	5	<0.1	28	19	116	62	19	14
		100 kV + 3 mm Al, SSD = 140 cm; 13 · 21	45	2	63	42	227	125	40	232
	PA	60 kV + 2.5 mm Al, SSD = 115 cm; 13 · 22	69	0.4	159	49	348	42	22	65
(1–4)	AP	65 kV + 2 mm Al, SSD = 120 cm; 18 · 24	135	0	233	187	904	628	227	192
	LLAT	70 kV + 3 mm Al, SSD = 115 cm; 13 · 24	289	34	299	187	844	511	93	45
	PA	65 kV + 2 mm Al, SSD = 120 cm; 18 · 24	168	0.4	411	140	858	111	37	13
(5–9)	PA	70 kV + 3 mm Al, SSD = 130 cm; 23 · 30	50	0	250	40	670	80	10	110
	LLAT	70 kV + 2.5 mm Al, SSD = 125 cm; 15 · 30	20	<0.1	70	30	210	130	30	5
(10–14)	PA	70 kV + 3 mm Al, SSD = 130 cm; 26 · 32	8	0	180	20	500	70	20	60
(15–19)	PA	80 kV + 2.5 mm Al, SSD = 140 cm; 34 · 36	10	0	330	10	650	80	10	50

Table 1B. Chest radiography in the adults: organ doses

Projection	Exposure parameters	Average absorbed doses (mGy)							
		Ovaries	Testes	RBM	LI	Lungs	Stomach	Breast	Thyroid
PA (normal tech.)	(sre) 80 kV + 3.5 mm Al, SSD = 140 cm; 36 · 36	0	0	0.10	0.003	0.21	0.03	0.005	0.005
PA (normal tech.)	(min) 70 kV + 4.5 mm Al, SSD = 130 cm; 36 · 36	0.001	0	0.11	0.002	0.25	0.03	0.005	0.005
PA (normal tech.)	(max) 75 kV + 1.0 mm Al, SSD = 130 cm; 36 · 36	0	0	0.93	0.01	2.01	0.17	0.04	0.05
LLAT (normal tech.)	(sre) 90 kV + 3 mm Al, SSD = 130 cm; 20 · 36	<0.001	0	0.20	0.005	0.31	0.22	0.08	0.01
PA (hartd tech.)	(sre) 110 kV + 3 mm Al, SSD = 160 cm; 36 · 36	<0.001	<0.001	0.17	0.006	0.43	0.06	0.04	0.10
PA (hard tech.)	(min) 125 kV + 5.5 mm Al, SSD = 155 cm; 40 · 34	0.008	0.003	0.15	0.008	0.37	0.06	0.001	0.009
PA (hard tech.)	(max) 115 kV + 4 mm Al, SSD = 170 cm; 36 · 36	0.01	<0.001	0.32	0.02	0.82	0.12	0.03	0.02

Table 2. Lung fluoroscopy and chest photofluorography in the adults: organ doses

Examination	Projection	Exposure parameters	Average absorbed doses (mGy)							
			Ovaries	Testes	RBM	LI	Lungs	Stomach	Breast	Thyroid
Lung fluoroscopy	AP	80 kV + 2.5 mm Al, SSD = 60 cm; 36 · 40	0.03	0.03	7.77	0.47	15.02	1.97	0.29	0.52
Photo-fluorography	PA	80 kV + 1 mm Al, SSD = 70 cm; 36 · 36	0.002	0	1.72	0.03	3.11	0.32	0.06	0.11

Table 3A. L-S spine radiography in children: organ doses

Age (years)	Projection	Exposure parameters	Average absorbed doses (μGy)							
			Ovaries	Testes	RBM	LI	Lungs	Stomach	Breast	Thyroid
(5–9)	AP	75 kV + 2.5 mm Al, SSD = 80 cm; 19 · 30	0.43	0.03	0.23	0.52	1.30	1.47	0.69	0.04
	LLAT	80 kV + 3.5 mm Al, SSD = 70 cm; 15 · 40	0.37	0.23	0.56	0.39	1.47	0.92	0.26	0.03
	RLAT	80 kV + 3.5 mm Al, SSD = 70 cm; 15 · 40	0.30	0.06	0.59	0.20	1.20	0.09	0.21	0.12
(10–14)	AP	80 kV + 2.5 mm Al, SSD = 80 cm; 23 · 32	2.15	0.21	0.68	2.27	1.20	5.90	0.48	0.003
	LLAT	90 kV + 3 mm Al, SSD = 70 cm; 17 · 32	1.60	0.92	1.70	2.11	1.21	5.02	0.10	0.03
	RLAT	90 kV + 3 mm Al, SSD = 70 cm; 17 · 32	2.15	0.13	1.83	1.10	0.98	0.41	0.25	0.03
(15–19)	AP	80 kV + 2.5 mm Al, SSD = 80 cm; 23 · 40	1.64	0.23	0.67	2.23	2.00	6.22	0.75	0.03
	LLAT	90 kV + 3 mm Al, SSD = 70 cm; 19 · 40	1.41	0.35	2.14	1.80	1.56	4.83	0.14	0
	RLAT	90 kV + 3 mm Al, SSD = 70 cm; 19 · 40	1.41	0.06	2.32	0.90	1.66	0.29	0.48	0.03

Table 3B. L-S spine radiography in the adults: organ doses

Projection	Exposure parameters	Average absorbed doses (mGy)							
		Ovaries	Testes	RBM	LI	Lungs	Stomach	Breast	Thyroid
AP	(aver) 90 kV + 3 mm Al, SSD = 80 cm; 35 · 40	3.24	0.35	0.90	4.37	0.78	10.76	0.29	0.004
	(min) 90 kV + 2 mm Al, SSD = 75 cm; 16 · 40	1.04	0.09	0.15	0.96	0.13	1.92	0.04	0
	(max) 90 kV + 3 mm Al, SSD = 70 cm; 27 · 37	13.64	0.76	2.68	14.50	1.66	36.58	0.48	0
LLAT	(aver) 100 kV + 4 mm Al, SSD = 75 cm; 20 × 40	0.88	0.21	1.40	1.36	0.18	3.29	0.02	0.02
	(min) 90 kV + 2 mm Al, SSD = 60 cm; 20 · 40	0.68	0.18	1.27	0.90	0.31	2.62	0.02	0.
	(max) 95 kV + 2.5 mm Al, SSD = 70 cm; 20 · 40	2.92	0.56	4.01	3.10	0.43	7.88	0.05	0
RLAT	(aver) 100 kV + 4 mm Al, SSD = 75 cm; 20 · 40	1.14	0.08	1.46	0.63	0.30	0.18	0.08	0.01
	(min) 90 kV + 2 mm Al, SSD = 60 cm; 20 · 40	0.64	0.12	1.34	0.42	0.27	0.08	0.09	0
	(max) 95 kV + 2.5 mm Al, SSD = 70 cm; 20 · 40	1.91	0.30	4.24	1.42	0.71	0.34	0.16	0

Table 4A. Thoracic spine radiography in children: organ doses

Age (years)	Projection	Exposure parameters	Average absorbed doses (μGy)							
			Ovaries	Testes	RBM	LI	Lungs	Stomach	Breast	Thyroid
(5–9)	AP	70 kV + 3 mm Al, SSD = 80 cm; 22 · 32	0.52	0	0.82	0.68	3.49	2.44	0.90	3.33
	LLAT	75 kV + 2.5 mm Al, SSD = 75 cm; 14 · 32	0.24	0.002	0.52	0.18	1.41	0.79	0.27	0.50
	RLAT	75 kV + 2.5 mm Al, SSD = 75 cm; 14 · 32	0.12	0	0.53	0.12	1.12	0.07	0.30	0.63
	PA (correction)	75 kV + 2.5 mm Al, SSD = 90 cm; 22 · 36	0.18	<0.001	0.44	0.15	0.88	0.12	0.03	0.10
(10–14)	AP	70 kV + 3 mm Al, SSD = 78 cm; 23 · 31	0.02	0	0.79	0.03	4.54	2.02	1.27	6.47
	LLAT	75 kV + 2.5 mm Al, SSD = 70 cm; 16 · 31	0.03	0	0.50	0.01	1.17	0.57	0.26	0.86
	RLAT	75 kV + 2.5 mm Al, SSD = 70 cm; 16 · 31	0	0	0.53	0.005	0.88	0.03	0.26	0.94
	PA (correction)	75 kV + 2.5 mm Al, SSD = 90 cm; 20 · 40	0.16	<0.001	0.30	0.10	0.82	0.10	0.02	0.06
(15–19)	AP	70 kV + 2.5 mm Al, SSD = 80 cm; 24 · 36	0	0	0.31	0.008	1.47	0.90	0.74	2.79
	LL	80 kV + 3.5 mm Al, SSD = 70 cm; 19 · 36	0.001	0	0.78	0.02	1.12	0.78	0.38	1.34
	LP	80 kV + 3.5 mm Al, SSD = 70 cm; 19 · 36	<0.001	0	0.81	0.008	0.92	0.03	0.40	1.29
	PA (correction)	75 kV + 2.5 mm Al, SSD = 100 cm; 24 · 53	0.16	<0.001	0.35	0.10	0.68	0.07	0.01	0.07

Table 4B. Thoracic spine radiography in the adults: organ doses

Projection	Exposure parameters	Average absorbed doses (mGy)							
		Ovaries	Testes	RBM	LI	Lungs	Stomach	Breast	Thyroid
AP	(aver) 80 kV + 3.5 mm Al, SSD = 81 cm; 25 · 38	<0.001	<0.001	0.43	0.007	2.50	0.97	0.79	4.87
	(min) 70 kV + 4.5 mm Al, SSD = 75 cm; 25 · 38	0	0	0.29	0.005	1.74	0.67	0.57	3.45
	(max) 85 kV + 3.5 mm Al, SSD = 70 cm; 26 · 38	0.005	0.03	5.91	0.14	35.44	13.22	11.25	67.73
LLAT	(aver) 90 kV + 3 mm Al, SSD = 70 cm; 20 · 38	0.009	0	3.87	0.06	5.89	3.21	1.61	8.64
	(min) 95 kV + 3.5 mm Al, SSD = 80 cm; 20 · 38	0.002	0	2.18	0.04	3.38	1.78	0.90	5.08
	(max) 90 kV + 3.5 mm Al, SSD = 60 cm; 20 · 38	0.04	0	16.26	0.29	24.05	13.31	6.59	45.88
RLAT	(aver) 90 kV + 3 mm Al, SSD = 70 cm; 20 · 38	0.004	0	3.96	0.03	4.67	0.09	1.57	8.71
	(min) 95 kV + 3.5 mm Al, SSD = 80 cm; 20 · 38	0	0	2.25	0.01	2.72	0.05	0.85	5.22
	(max) 90 kV + 3.5 mm Al, SSD = 60 cm; 20 · 38	0	0.001	16.56	0.13	19.19	0.42	6.58	37.43

Table 5. Abdomen radiography in the adults: organ doses

Projection	Exposure parameters	Average absorbed doses (mGy)							
		Ovaries	Testes	RBM	LI	Lungs	Stomach	Breast	Thyroid
AP	(aver) 80 kV + 4.5 mm Al, SSD = 75 cm; 36 · 43	2.66	1.02	1.02	2.59	0.41	5.93	0.15	0.02

Table 6. Examination of stomach and oesophagus in the adults: organ doses

Projection	Exposure parameters	Average absorbed doses (mGy)							
		Ovaries	Testes	RBM	LI	Lungs	Stomach	Breast	Thyroid
PA	Scopy (aver) 80 kV + 2.5 mm Al, SSD = 45 cm; 30 · 34	4.85	<0.001	11.19	4.66	14.79	5.07	0.42	0
	Radiograph 1 80 kV + 2.5 mm Al, SSD = 45 cm; 18 · 24	0.26	0	2.09	0.88	1.02	2.14	0.04	0
	Radiograph 2 80 kV + 2.5 mm Al, SSD = 45 cm; 24 · 24	0.50	0.001	2.75	1.07	1.19	2.20	0.05	0

Table 7A. Barium enema in the adults: organ doses

Projection	Exposure parameters	Average absorbed doses (mGy)							
		Ovaries	Testes	RBM	LI	Lungs	Stomach	Breast	Thyroid
AP	Scopy 80 kV + 2.5 mm Al, SSD = 50 cm; 34 · 34	6.65	3.49	1.78	7.60	0.12	11.68	0.02	0.004
	Radiograph 1 80 kV + 2.5 mm Al, SSD = 50 cm; 40 · 35	6.51	3.72	2.37	8.01	0.18	13.74	0.05	0
	Radiograph 2 80 kV + 2.5 mm Al, SSD = 50 cm; 30 · 24	6.80	40.97	1.17	5.53	0.006	0.20	0	0
	Radiograph 3 80 kV + 2.5 mm Al, SSD = 50 cm; 24 · 18	5.66	0.27	0.58	4.52	0.006	0.26	0.001	0
	Radiograph 4 80 kV + 2.5 mm Al, SSD = 50 cm; 24 · 18	6.96	0.35	0.73	6.78	0.008	0.57	0.0002	0

Table 7B. Barium enema in children: organ doses. (Exposure conditions as found in the Polish Mother Memorial Hospital in Łódź)

Age (years)	Projection	Exposure parameters	Average absorbed doses (μGy)							
			Ovaries	Testes	RBM	LI	Lungs	Stomach	Breast	Thyroid
(10–14)	AP	Radiograph 70 kV + 3 mm Al, SSD = 100 cm; 22 · 26	0.58	0.23	0.21	0.55	0.16	1.16	0.04	<0.001
(15–19)	AP	Radiograph 80 kV + 3 mm Al, SSD = 100 cm; 26 · 36	0.65	0.32	0.39	0.77	0.81	1.94	0.37	<0.001

Table 8. Cystourethrography in children: organ doses. (Exposure conditions as found in the Polish Mother Memorial Hospital in Łódź)

Age (years)	Projection	Exposure parameters	Average absorbed doses (μGy)							
			Ovaries	Testes	RBM	LI	Lungs	Stomach	Breast	Thyroid
<1	AP	63 kV + 3 mm Al, SSD = 100 cm; 12.6 · 24.0	0.15	0.84	0.21	0.20	0.65	0.41	0.15	0.03
(1–4)	AP	63 kV + 3 mm Al, SSD = 100 cm; 17 · 24	0.12	0.76	0.09	0.14	0.17	0.34	0.07	0.006
(5–9)	AP	70 kV + 3 mm Al, SSD = 100 cm; 22 · 30	0.48	2.05	0.26	0.55	0.37	1.16	0.11	<0.001
(10–14)	AP	70 kV + 3 mm Al, SSD = 100 cm; 26 · 30	0.41	1.50	0.15	0.7	0.04	0.98	0.01	0
(15–19)	AP	77 kV + 3 mm Al, SSD = 90 cm; 30 · 40	0.50	0.96	0.21	0.58	0.10	1.48	0.03	<0.001

Table 9. Urography (IVU): organ doses

Age (years)	Projection	Exposure parameters	Average absorbed doses (μGy)							
			Ovaries	Testes	RBM	LI	Lungs	Stomach	Breast	Thyroid
<1	AP	60 kV + 2.5 mm Al, SSD = 90 cm; 13 · 20	0.19	0.04	0.22	0.24	0.84	0.50	0.13	0.06
(1–4)	AP	70 kV + 2 mm Al, SSD = 90 cm; 17 · 23	0.53	0.26	0.43	0.66	1.20	1.56	0.37	0.04
(5–9)	AP	70 kV + 2 mm Al, SSD = 90 cm; 22 · 26	0.76	0.26	0.30	0.78	0.21	1.94	0.05	0.01
(10–14)	AP	70 kV + 2 mm Al, SSD = 90 cm; 26 · 36	1.04	0.71	0.59	1.13	1.24	3.08	0.38	<0.001
(15–19)	AP	80 kV + 2.5 mm Al, SSD = 80 cm; 30 · 40	2.04	1.03	0.86	2.18	0.52	5.69	0.15	<0.001
(10–14)	AP	70 kV + 2 mm Al, SSD = 90 cm; 26 · 36	1.04	0.71	0.59	1.13	1.24	3.08	0.38	<0.001
Adults	AP	80 kV + 3.5 mm Al, SSD = 75 cm; 30 · 40 (aver)	0.76	0.36	0.17	0.97	0.05	2.35	0.02	0
	AP	80 kV + 2.5 mm Al, SSD = 75 cm; 35 · 43 (min)	0.79	3.79	0.30	0.96	0.06	2.28	0.02	0.009
	AP	70 kV + 3 mm Al, SSD = 75 cm; 35 · 43 (max)	5.49	22.05	2.09	6.60	0.41	14.67	0.14	0

Table 10. Pelvis and hip joints radiography: organ doses

Age (years)	Projection	Exposure parameters	Average absorbed doses (μGy)							
			Ovaries	Testes	RBM	LI	Lungs	Stomach	Breast	Thyroid
<1	AP	60 kV + 2.5 mm Al, SSD = 80 cm; 12.7 · 20.0	0.12	1.04	0.15	0.19	0.07	0.39	0.02	<0.001
(1–4)	AP	60 kV + 3.5 mm Al, SSD = 85 cm; 17.7 · 22.0	0.14	0.91	0.08	0.17	0.009	0.28	<0.001	0
(5–9)	AP	70 kV + 2 mm Al, SSD = 85 cm; 23 · 30	0.79	4.22	0.37	0.78	0.02	1.13	<0.001	<0.001
(10–14)	AP	70 kV + 3 mm Al, SSD = 85 cm; 28 · 35	0.93	4.58	0.49	1.11	0.03	1.50	<0.001	0
(15–19)	AP	80 kV + 3 mm Al, SSD = 80 cm; 34 · 37	1.01	7.52	0.54	1.34	0.01	0.86	0.007	<0.001
Adults	AP	(aver) 80 kV + 3.5 mm Al, SSD = 80 cm; 40 · 44	0.52	3.16	0.24	0.57	0.003	0.36	<0.001	0
	AP	(min) 80 kV + 3.5 mm Al, SSD = 80 cm; 40 · 30	0.33	2.39	0.12	0.37	<0.001	0.02	<0.001	0
	AP	(max) 85 kV + 3.5 mm Al, SSD = 70 cm; 40 · 30	11.53	53.63	3.84	11.80	0.02	1.04	<0.001	0

Table 11. Effective doses to patients from X-ray examinations analysed in this paper

Type of examination	Age of patients (years)	DEF/AK* (mSv/mGy)	Mean value of DEF for the whole examination (mSv)
Chest radiography	<1	AP – 0.8392±0.0287	0.10
		PA – 0.7973±0.0205	
	(1–4)	AP – 0.6351±0.0151	0.30
		PA – 0.4920±0.0068	
		LLAT – 0.3673±0.0065	
	(5–9)	PA – 0.2816±0.0057	0.23
		LLAT – 0.3552±0.0063	
	(10–14)	PA – 0.2674±0.0044	0.13
	(15–19)	PA – 0.2635±0.0035	0.17
	Adults	PA^{N} (normal technique) – 0.2705±0.0020	
		PA^{T} (hard technique) – 0.3051±0.0024	0.11
		LLAT – 0.1187±0.0011	
Lung fluoroscopy	Adults	PA – 0.1034±0.0009	4.10
Chest photofluorography	Adults	PA – 0.1181±0.0011	0.82
L-S spine radiography	(5–9)	AP – 0.3596±0.0079	
		LLAT – 0.2415±0.0051	1.17
		RLAT – 0.1780±0.0055	
	(10–14)	AP – 0.2095±0.0043	
		LLAT – 0.0931±0.0013	3.56
		RLAT – 0.0667±0.0015	
	(15–19)	AP – 0.1662±0.0024	
		LLAT – 0.0674±0.0008	3.68
		RLAT – 0.0519±0.0010	
	Adults	AP – 0.1458±0.0019	
		LLAT – 0.0574±0.0007	4.33
		RLAT – 0.0429±0.0008	
Thoracic spine radiography	(5–9)	AP – 0.2989±0.0085	
		LLAT – 0.2201±0.0060	1.04
		RLAT – 0.1713±0.0062	
		PA – 0.3423±0.0068	
	(10–14)	AP – 0.2067±0.0056	
		LLAT – 0.1287±0.0034	1.05
		RLAT – 0.1010±0.0034	
		PA – 0.2622±0.0042	
	(15–19)	AP – 0.2231±0.0064	
		LLAT – 0.0904±0.0025	0.62
		RLAT – 0.0741±0.0025	
		PA – 0.2196±0.0039	
	Adults	AP – 0.2066±0.0045	
		LLAT – 0.0705±0.0023	3.03
		RLAT – 0.0579±0.0015	
Abdomen radiography	Adults	AP – 0.1375±0.0018	2.18

Table 11 contd

Type of examination	Age of patients (years)	DEF/AK* (mSv/mGy)	Mean value of DEF for the whole examination (mSv)
Stomach and oesophagus examination	Adults	PA – scopy – 0.0479±0.0003 PA – radiograph 1 – 0.0178±0.0001 PA – radiograph 2 – 0.0213±0.0001	14.00
Barium enema	Adults	AP – scopy – 0.0748±0.0009 AP – radiograph 1 – 0.0787±0.0015 AP – radiograph 2 – 0.0947±0.0008 AP – radiograph 3 – 0.0309±0.0006 AP – radiograph 4 – 0.0324±0.0005	22.73
Urography (IVU)	<1	AP – 0.8119±0.0206	0.96
	(1–4)	AP – 0.4161±0.0099	2.31
	(5–9)	AP – 0.2699±0.0042	2.80
	(10–14)	AP – 0.2839±0.0048	5.08
	(15-19)	AP – 0.1740±0.0022	8.08
	Adults	AP – 0.1554±0.0018	3.08
Pelvis and hip joints radiography	<1	AP – 0.7167±0.0108	0.26
	(1–4)	AP – 0.4879±0.0046	0.21
	(5–9)	AP – 0.3531±0.0036	0.94
	(10–14)	AP – 0.2486±0.0030	1.14
	(15–19)	AP – 0.2106±0.0024	1.42
	Adults	AP – 0.2398±0.0027	0.61

* DEF/AK – values of effective dose (DEF) per unit of entrance air kerma (AK), values given here concern one exposure in the specified projection.

Collective effective doses as a basis for assessing patients' risk

The results obtained can be summarised by estimating collective doses resulting from the overall number of X-ray examinations.

Thus, the results of the evaluation concerning the number of examinations have to be combined with those expressing effective patient doses in particular examinations. The sum of collective effective doses in all types of examinations is the basis for assessing radiation risk resulting from diagnostic radiology at large. The number of patients undergoing individual examinations are given in Table 12.

Average effective patient doses in **interventional radiology** procedures (Table 13) were estimated on the basis of the author's own results of measurements and computations; four types of procedures were analysed as performed in 3 clinical hemodynamic departments in Łódź. All procedures were performed using SIEMENS devices, with pulse or constant potential generators. The 'doses' were measured in adult patients during coronary angiography, the angiographies of spine arteries, renal arteries, and sclerotherapy of testicular varices. TLDs were used for measuring the entrance air kerma on the patients. Dosemeters were placed at 10 constant anatomical body points; procedure protocols (time of particular projections, direction of primary beam, etc.) were recorded. The highest value of

kerma was found in angiography of renal arteries (100 mGy). The measurement data were used for further computation of effective doses (by Monte Carlo simulation) performed for coronary angiographies, the most frequent procedure. It was found that the effective dose per unit of the entrance air kerma ranged from 0.03 mSv/mGy to 0.07 mSv/mGy. The highest value was obtained for PA projection and the lowest for lateral projection performed with additional filtration 0.1 mm Cu.

The estimation of the average effective dose to patients in interventional radiology procedures was based on the following two assumptions:

(a) the highest value of effective dose per unit of the entrance air kerma found for coronary angiography (0.07 mSv/mGy) may be adopted as a reasonable approximation for all patients in interventional radiology, and

(b) the highest value of the entrance air kerma measured in all the procedures (100 mGy) may be adopted as a reasonable approximation of an average exposure of patients in interventional radiology.

Taking these assumptions into account, the average effective dose to adult patients in interventional procedures was estimated as 7 mSv.

Table 12. The number of X-ray examinations in Poland in 1986 and 1995

Type of examinations	1986		1995	
	Annual number in thousands	% of total number	Annual number in thousands	% of total number
Basic X-ray examinations:				
– head	1620	7.6	1770	6.4
– dental	1200	5.6	2870	10.3
– photofluorography of chest	5860	27.5	6990	25.3
– remaining chest examinations	4870	22.8	5760	20.9
– abdomen and GI tract	1330	6.2	910	3.3
– stomach and duodenum	400	1.9	400	1.4
– barium enema	46	0.2	90	0.3
– genital – urinary system	340	1.6	300	1.1
– urography	310	1.5	230	0.8
– spine	2540	11.8	3620	13.1
– upper limbs	1380	6.5	2160	7.8
– lower limbs	2045	9.6	2570	9.3
– hip-joint radiography	450	2.1	580	2.1
Basic exam. – total	21200	99.4	26900	97.5
In this number: examinations with fluoroscopy	2000	9.4	590	2.2
Specialised examinations:				
– with contrast application (angiographies etc.)	84	0.4	110	0.4
– CT	38	0.2	170	0.6
– interventional radiology	–	–	32	0.1
– mammography	–	–	280	1.0
– bone densitometry	–	–	37	0.1
Specialised examinations – total	120	0.6	630	2.3
X-ray examinations – total	21400	100	27600	100

As irradiation of patients in these procedures may vary largely (dependending on the clinical needs and the degree of difficulty), the evaluated dose should be taken as a first approximation only, allowing to use it for estimating the share of interventional radiology in the overall irradiation from X-ray diagnostics in Poland.

For X-ray examinations in exposure conditions significantly different from conventional ones, the values of average effective doses were taken from the literature (2,8,9,11). The average dose for CT procedures was evaluated on the basis of the British data (8) bearing in mind that of the total number of procedures, head and abdomen CT examinations make about 70% and 30%, respectively.

Table 13. Collective effective doses resulting from particular X-ray examinations performed in 1995

Type of examination	Share of the total number of X-ray examinations (%)	Collective effective dose (man-Sv)		
		children	adults	Total
Chest radiography	20.77	120	575	695
Lung fluoroscopy	0.35	(–)	402	402
Chest photofluorography	25.32	(–)	5732	5732
Thoracic spine radiography	7.60	396	5012	5408
L-S spine radiography	5.10	169	5880	6049
Pelvis and hip joints radiography	2.70	115	353	468
Urography (IVU)	0.85	135	619	754
Cystourethrography	0.25	95	(–)	95
Abdomen radiography	1.53	44	826	870
Examinations of stomach and oesophagus	1.44	51	5348	5399
Barium enema	0.33	(–)	2066	2066
Conventional head examinations	6.42	24	157	181
Dental examinations	10.28	39	251	290
Radiographies of upper extremities (hands)	7.60			40*
Radiographies of lower extremities (legs)	7.20			40*
Conventional contrast examinations	0.37			2700*
Interventional radiology	0.11			220*
Mammography	1.03	(–)	283	283**
Computed tomography (CT)	0.62			600**
Bone densitometry	0.13			<1*
All X-ray examinations	100			32292

(–) examination rarely performed in this age group,
* estimated values,
** values taken from the literature (8,11).

Table 13 summarises collective effective patient doses from X-ray examinations performed in 1995, and Tables 14A (adults) and 14B (children and adolescents) in 1986 and 1995.

The mean effective doses per one examination were as follows:
- for adult patients: 1.45 mSv in 1986 year, and 1.21 mSv in 1995 year,
- for patients under 19: 0.74 mSv in 1986 year, and 0.65 mSv in 1995 year.

Table 14A. Collective effective doses for adult patients: the 1986 and 1995 results

Type of examination	1986		1995	
	annual number (in thousands)	collective effective dose (man-Sv)	annual number (in thousands)	collective effective dose (man-Sv)
Chest radiography	4238	466	5073	558
Lung fluoroscopy	900	3690	98	402
Chest photofluorography	5337	4376	6990	5732
Spine radiography	2282	8400	3012	10892
Extremities radiography	2975	60	4150	83
Abdomen radiography	800	1744	379	826
Examinations of stomach and oesophagus	400	5600	382	5348
Barium enema	50	1137	91	2068
Urography (IVU)	260	801	235	724
Pelvis and hip joints radiography	244	151	579	359
Conventional head examinations	982	98	1568	157
Dental examinations	986	99	2510	251
Computed tomography (CT)	37	130	171	599
Special contrast examinations	66	1650	109	2725
Total	19557	28402	25347	30724

Table 14B. Collective effective doses to patients under 19: the 1986 and 1995 results

Type of examination	1986		1995	
	annual number (in thousands)	collective effective dose (man-Sv)	annual number (in thousands)	collective effective dose (man-Sv)
Chest radiography	633	113	665	120
Spine radiography	253	491	496	565
Pelvis and hip joint radiography	204	81	174	115
Abdomen radiography	50	67	42	44
Cystourethrography and IVU	83	285	104	230
Conventional head examinations	221	27	204	24
Total	1444	1064	1685	1098

For obvious reasons the estimations include some errors resulting from:
- the absorbed energy computations by Monte Carlo simulation ($\leqslant 4$),
- the theoretically computed values of the entrance air kerma (40), and
- the questionnaire method used for the collection of data on the number of X-ray examinations (13% in 1986, and 10% in 1995).

Hence, estimated 42% and 41% of errors for 1986 and 1995, respectively in average effective doses per examination and *per capita*.

In conclusion, the estimated indicators of exposure levels in Poland are as follows:
- the average effective dose per examination: (1.4 ± 0.6) mSv in 1986, (1.2 ± 0.5) mSv in 1995,
- the average effective dose *per capita*: (0.8 ± 0.3) mSv in 1986 and 1995.

REFERENCES

1. Beck TJ, Rosenstein M. Quantification of Current Practice in paediatric Roentgenography for Organ Dose Calculations. HEW Publication (FDA) 79-8087. Bureau of Radiological Health, Rockville, Maryland, 1979.
2. Bezakova E, Collins PJ, Beddoe AH. Absorbed dose measurements in dual energy X-ray absorptiometry (DXA). Br J Radiol 70: 172–179,1997.
3. Cristy M. Mathematical phantoms representing children of various age for use in estimates of internal dose. NUREGICR-1159. Oak National Laboratory Rep., ORNL/NUREG/TM-367, 1980.
4. Drexler G, Panzer W, Widenmann L et al. The calculation of dose from external photon exposure using reference human phantoms and Monte Carlo methods. Part III: Organ doses in X-ray diagnosis. GSF-Bericht, Munchen, 1984.
5. Jones DG, Wall BF. Organ doses from medical X-ray examinations calculated using Monte Carlo techniques. NRPB Publication NRPB-R186, Chilton, 1985.
6. Rosenstein M. Organ doses in diagnostic radiology. HEW Publication (FDA) 76-8030. Bureau of Radiological Health, Rockville, 1979.
7. Seelentag WW, Panzer W, Drexler G et al. A catalogue of spectra for the calibration of dosemeters. GSF-Bericht, Munchen, 1979.
8. Shrimpton PC, Jones DG, Hillier MC. Survey of CT Practice in the UK. Part 2: Dosimetric Aspects. NRPB-R249, National Radiological Protection Board, Chilton, Didcot, 1991.
9. Sorenson JA. Relationship between patient exposure and measurement precision in dual-photon absorptiometry of the spine. Phys Med Biol 36: 169–176, 1991.
10. Staniszewska MA. A modification of Cristy's mathematical human phantoms for Monte Carlo simulation. J Radiol Prob 12 (2): 85–92, 1992.
11. UNSCEAR 1993 Report, United Nations, New York, 1993.

Received for publication: August 13, 1999
Approved for publication: November 15, 1999